Publication P4

Sami Ruoho and Antero Arkkio. 2008. Partial demagnetization of permanent magnets in electrical machines caused by an inclined field. IEEE Transactions on Magnetics, volume 44, number 7, pages 1773-1778.

Partial Demagnetization of Permanent Magnets in Electrical Machines Caused by an Inclined Field

Sami Ruoho[1,2] and Antero Arkkio[1]

[1]Laboratory of Electromechanics, Helsinki University of Technology, FIN-02015 TKK, Finland
[2]Neorem Magnets Oy, FIN-28400 Ulvila, Finland

We report a study of partial demagnetization of axially pressed sintered Nd–Fe–B magnets by inclined pulse demagnetization measurements, including a recoil behavior of the Nd–Fe–B material. From these measurements, we develop a simple empirical model for demagnetization of Nd–Fe–B magnets caused by an inclined field. We calculate demagnetization of a simple surface-magnet machine and a two-pole high-speed machine by using an exponent function-based model, taking also the inclined demagnetizing field into account. We show that it is not enough to consider only antiparallel demagnetizing field components in accurate demagnetization calculations.

Index Terms—**Demagnetization, finite-element analysis, magnetic field modeling, permanent magnets, synchronous machines.**

I. Introduction

RECENT models for demagnetization of Nd–Fe–B permanent magnets in permanent-magnet machines take into account only one field component: the demagnetizing field directly against the magnetization direction [1], [2], the antiparallel field. Thus, it is assumed that only the magnetic field component against the magnetization direction matters. With this assumption, the demagnetization resistance of Nd–Fe–B magnet should have a $1/\cos\varphi$ dependence on the field inclination, where φ is the angle between the magnetization direction and the applied field (Fig. 1). This assumption also means that the field perpendicular to magnetization direction should not cause any demagnetization.

In reality, $1/\cos\varphi$ dependence is not a proper assumption when modeling a demagnetization of mass-produced Nd–Fe–B magnets caused by an inclined field, as will be shown later in this paper. The reason for this is that the mass-produced Nd–Fe–B magnets do not have a perfect grain orientation, and thus, they are more prone to demagnetization. The $1/\cos\varphi$ dependence would also mean a perfect demagnetization resistance against infinite field when $\varphi = 90°$, which is not reasonable.

Katter [3] has made a good research of angular dependence of demagnetization stability for the magnets used in some scientific research equipment. He has also compared different pressing methods, which do give different orientation degrees of the grains inside the magnetic material. According to the publication by Martinek and Kronmüller [4], the increase of orientation degree increases the demagnetization resistance against an inclined field.

This paper first presents measurement results from tests, in which Nd–Fe–B magnet samples have been demagnetized by an inclined field. Based on these measurements, a simple model is presented to take into account the angular dependence of demagnetization resistance when modeling demagnetization of permanent magnets in electrical machines. A model is implemented in a finite-element-method (FEM) calculation and used to calculate the demagnetization of two generic permanent-magnet machines when heavily loaded and overheated.

Digital Object Identifier 10.1109/TMAG.2008.921951

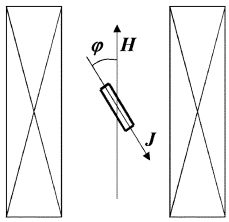

Fig. 1. Experimental setup of the pulsed field measurements. The sample was set in a special jig in a magnetizing fixture. The jig could be adjusted to different angles φ. The field H was applied with a magnetizing fixture as a pulse field. The self demagnetizing field caused by the sample magnetic polarization J was not taken into account due to the sample shape with very low demagnetizing factor.

II. Demagnetization of Nd–Fe–B Magnet Material by an Inclined Field

In this section, the samples and measuring equipment used in the pulsed field measurements are described. The results acquired by these measurements are presented. The recoil behavior of sintered Nd–Fe–B material is also briefly presented.

A. Samples

Three different Nd–Fe–B magnet grades were tested. All grades were axially pressed commercial grades with some 92% orientation degree. The orientation degree was tested with a method presented by Fernengel *et al.* [5]. Cylindrical samples of two different sizes were manufactured: large ones with diameters of 18 mm and heights of 5 mm, and small ones with diameters of 4 mm and heights of 20 mm. All the samples were magnetized axially, through the thickness. The samples were wire-cut from larger block magnets. The large samples $(\mathrm{D}18 \times \underline{5})$ were used for hysteresisgraph measurements and the small samples $(\mathrm{D}4 \times \underline{20})$ for pulsed field measurements.

B. Hysteresisgraph Measurements

In the hysteresisgraph measurement a sample is placed in a large electromagnet, which generates a homogenous field exactly antiparallel to the direction of the magnetic polarization. The demagnetizing field is then slowly increased, and the magnetic polarization (J) and the demagnetizing field (H) values are measured and stored during the course of measurement. With this method, the whole second quadrant hysteresis-curve

TABLE I
HYSTERESISGRAPH MEASUREMENT RESULTS

Sample	Sample type	B_r (T)	$_JH_c$ (kA/m)	$H_{k,90\%}$ (kA/m)
A	● High B_r	1.32	1050	910
B	▲ Medium B_r	1.22	1635	1470
C	■ Medium high $_JH_c$	1.17	2080	1580

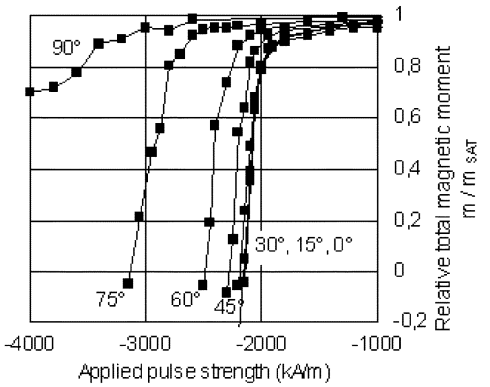

Fig. 2. Relative total magnetic moment of sample C as a function of the applied pulse strength. The measurements are done after each pulse with Helmholtz coil. Different curves are for different angles between the magnetic polarization axis and demagnetization pulse.

is easily acquired. The hysteresisgraph measurement method is described more thoroughly in [6].

The hysteresisgraph measurements were performed with a Walker Scientific MH1575PS hysteresisgraph. The results of the measurements of the samples used in this paper are presented in Table I. The values of B_r,$_J H_c$, and $H_{k,90\%}$ in a room temperature are given. $H_{k,90\%}$ means the demagnetizing field strength H_k, where the magnetic polarization J of the sample has been decreased by 10%.

C. Pulsed Field Measurements

The shape of samples for pulsed field measurements was selected so that the self-demagnetization factor of the samples is as low as possible, so that the self-demagnetizing field of the samples can be ignored in calculations. That is why the pulsed field measurements were performed on the samples resembling a long needle shape, which has a zero self-demagnetizing factor. The shape of diameter of 4 mm and length of 20 mm was selected, because it is close enough the "long needle" shape and because this shape and size is practical to handle.

The demagnetizing pulses were applied on the samples with a pulse magnetizer giving a pulse shape of a half sine-wave. The pulse length was 4 ms. The accuracy of the magnetizer on the pulse strength is $\pm 2\%$. The total magnetic moment of each sample was first measured with a Helmholtz coil, which has the measurement accuracy of $\pm 1\%$. Then, a series of pulses with increasing field strength was applied on the sample. The samples were measured with the Helmholtz coil after each pulse. The series of pulses were repeated keeping the sample at different angles with the applied field using a special plastic jig. The measurement setup is shown in Fig. 1.

Three samples (A, B, and C) were used. The measurement results for sample C are shown in Fig. 2.

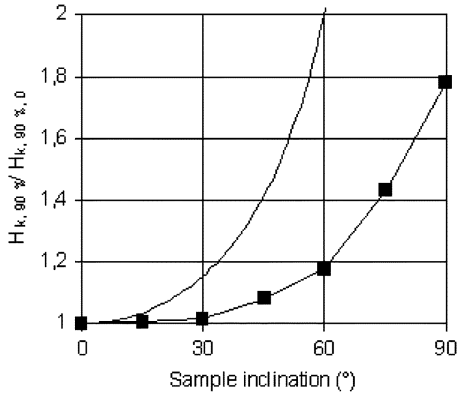

Fig. 3. Relative field strength needed to reduce the magnetic polarization of sample C by 10% as a function of sample inclination. Solid line is a $1/\cos\varphi$ curve showing the difference to the measured values (black rectangles). The data for this figure is based on the measurement results shown in Fig. 2.

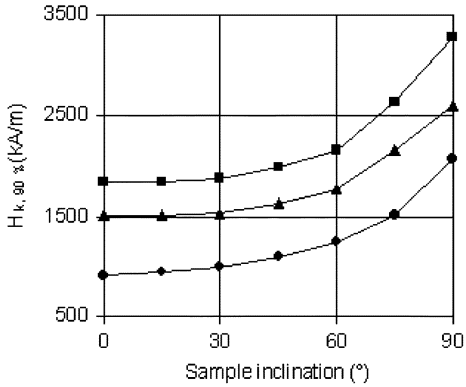

Fig. 4. Field strength needed to reduce the magnetic polarization of the three samples by 10% as a function of sample inclination. This data is based on the pulsed field measurements. (Circles: Sample A, Triangles: Sample B, Rectangles: Sample C).

Fig. 3 is generated using the data of Fig. 2. Fig. 3 shows how much field is needed to reduce the magnetic polarization by 10% as a function of sample inclination. The required field is shown related to the field required to drop the sample magnetic polarization by 10% with zero inclination. The inverse cosine curve is also shown for comparison purposes. It can clearly be seen that the assumption of the $1/\cos\varphi$ dependence is not satisfying when modeling the demagnetization of axially pressed Nd–Fe–B magnets by inclined fields. Fig. 4 shows for all the samples the required field to drop the magnetic polarization by 10% as a function of sample inclination.

D. Recoil Behavior of Nd–Fe–B Samples

In literature, the shape of a recoil curve is normally assumed to be a straight line. This assumption can be seen in many papers using irreversible demagnetization models implemented in FEM analysis [1], [2]. However, the recoil curve of Nd–Fe–B magnet material can be estimated with a straight line only, when demagnetization causes only a small loss of magnetic polarization [7].

In Fig. 5, a hysteresis curve and a drop of polarization by independent pulses are shown for the sample A. It can be seen that a curve acquired by a set of pulses crosses the horizontal axis a bit further on negative H-axis than the hysteresis curve measured

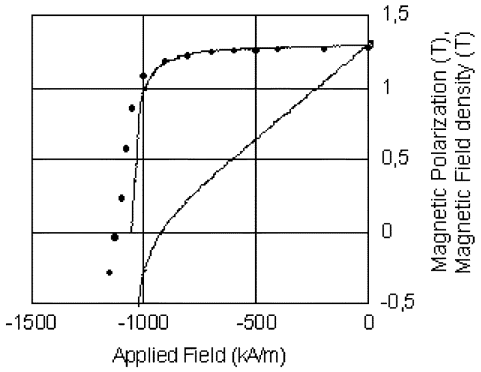

Fig. 5. Second quadrant hysteresis curve measured with a hysteresisgraph (solid line) and a drop of magnetic polarization of sample A with zero inclination as a function of applied pulse strength (single dots). The single dots are acquired by measuring the total magnetic moment of the sample with a Helmholtz coil after each demagnetizing pulse.

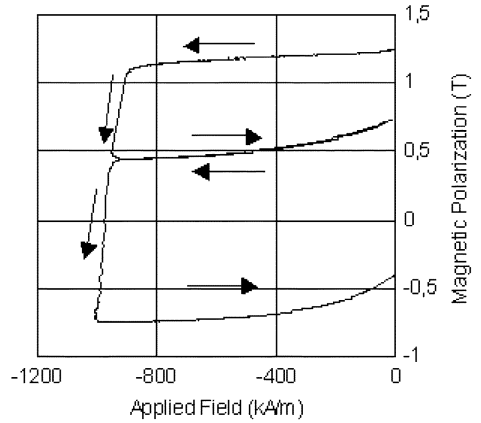

Fig. 6. Curve measured with a hysteresisgraph showing recoil behavior of Nd–Fe–B magnet material. The field is first increased on the negative H-axis. After some demagnetization, the field is decreased to zero. After that the field is again increased to cause more demagnetization. It can be seen that the recoil curve is clearly bent and that there is no significant minor loop in Nd–Fe–B recoil curve. The arrows show the course of the measurement.

with a hysteresisgraph. The reason for this can be seen in Fig. 6: The recoil curve of Nd–Fe–B magnet is not a straight line but curves clearly upwards near the vertical axis. It can also be seen that there is no significant minor loop in Nd–Fe–B magnet recoil behavior, which is exactly what could be expected according to Harland *et al.* [8].

In pulse demagnetization measurements, the magnetic polarization of the sample is measured after each demagnetizing pulse with the Helmholtz coil. After the pulse, the sample has returned to its original working line. Because the recoil curve is bent upwards, the magnetic polarization has increased after the pulse. The magnetic polarization in hysteresisgraph measurement, however, is measured simultaneously when the field is applied to a sample. So there is no recoil operation during the hysteresisgraph measurement.

When comparing the intersection points with the horizontal axis, the self-demagnetization field will be zero because J is zero on the axis, which means that the self-demagnetizing field can be ignored. Thus, the only demagnetizing field is the external applied field, when crossing the horizontal axis.

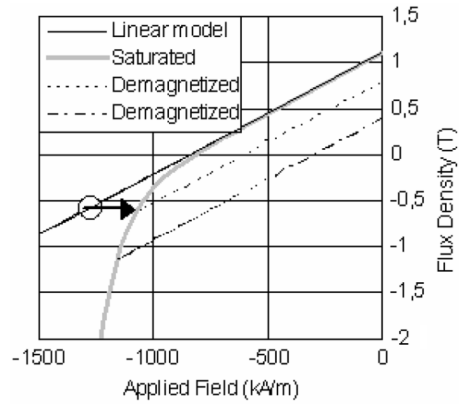

Fig. 7. Calculated curve of an irreversible demagnetization of Nd–Fe–B magnet modeled with the exponent function model. The working point (circle in figure), which is calculated using the linear model, is reduced to a curve described by the exponent function, if the working point is too far on the negative H -axis. The saturated curve is drawn according to (1) [2], [10].

This comparison of the hysteresisgraph and pulse field measurements (Fig. 5) clearly shows that the pulsed field measurement cannot be used to define the intrinsic coercivity of a magnet material accurately if the shape of the recoil curve is not known (Fig. 6).

III. Model

In this section, an empirical model for modeling of demagnetization caused by an inclined field is presented based on the measurement results presented in the previous section.

A. Modeling Demagnetization With Antiparallel Field

In paper [2], Ruoho *et al.* have presented an exponential function based model, in which the sharpness of the HB-curve knee can be adjusted with parameter K_1 in (1), whereas K_2 is calculated based on ${}_JH_c$ and B_r [2]. This model is used accordingly. During FEM calculations, a working point of each element containing permanent magnet material is checked after each time step against the model according to Fig. 7. Only the magnetic field component antiparallel to the magnetization direction is considered. If the working point in the element is too far on the negative H-axis, the remanence of that element is reduced. If there has been any demagnetization in any element according to the model, the field for the time-step is recalculated

$$B = B_\mathrm{r} + \mu_0\mu_\mathrm{r}H - \mathrm{E}e^{\mathrm{K}_1(\mathrm{K}_2+H)}. \tag{1}$$

More thorough information concerning this demagnetization model can be found in paper [2].

B. Demagnetization With Inclined Field

In this paper, the effect of demagnetizing field inclination is taken into account in FEM analysis. A third-order polynomial is first fitted into the data in Fig. 8 taking into account only samples B (triangles) and C (rectangles). This is because the magnet grade used in the modeled machine has magnetic properties between those two samples, which can be seen in Tables I and II. Also, several kinds of other functions were fitted to the data, including the polynomials of different orders. The best fit was ac-

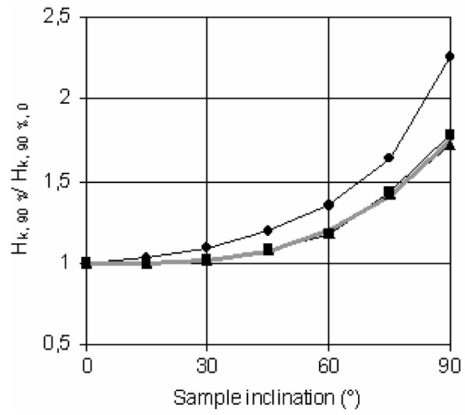

Fig. 8. Relative field strength needed to reduce 10% of magnetic polarization of a sample as a function of sample inclination for all three samples. The gray curve shows the fitted curve according to (2). The measured points are based on the pulsed field measurements.

TABLE II
MAIN PARAMETERS OF THE MODELED MACHINES

Parameter:	Motor 1	Motor 2
Number of poles	4	2
Outer diameter of the stator	310 mm	70 mm
Air gap diameter	200 mm	33.5 mm
Core length	246 mm	30 mm
Number of stator slots	48	18
Connection	Star	Star
Input frequency	50 Hz	900 Hz
Rated voltage (phase-to-phase)	400 V	690 V
Rated power	40 kW	8.5 kW
B_r of PM material at 20 ºC	1.2 T	1.2 T
${}_JH_c$ of PM material at 20 ºC	-1750 kA/m	-1750 kA/m
B_r of PM material at 150 ºC	1.0 T	1.0 T
${}_JH_c$ of PM material at 150 ºC	-440 kA/m	-440 kA/m

quired using the third-order polynomial, which still gives quite a simple equation:

$$ {}_JH_c^{\mathrm{ANG}} = {}_JH_c\left(1 + a_1\varphi + a_2\varphi^2 + a_3\varphi^3\right). \qquad (2) $$

In this case, the parameters in (2) are as follows: $a_1 = +3.17 \cdot 10^{-4}\ \mathrm{deg}^{-1}$, $a_2 = -3.38 \cdot 10^{-5}\ \mathrm{deg}^{-2}$ and $a_3 = +1.37 \cdot 10^{-6}\ \mathrm{deg}^{-3}$.

It is assumed that ${}_JH_c$ has the same dependence on the angle, as $H_{k,90\%}$, which is shown in Fig. 8.

After each time step in time-stepping FEM modeling, the demagnetizing field inclination φ and field magnitude is acquired from FEM solution. The intrinsic coercivity ${}_JH_c$ is adjusted according to the polynomial in (2), and the field magnitude, not just the antiparallel component, is compared against the exponential model using the adjusted intrinsic coercivity ${}_JH_c^{\mathrm{ANG}}$. If there is any new demagnetization in any element consisting of permanent-magnet material during the time step, the field is recalculated for that time step and the checking is made again, until there is no further demagnetization.

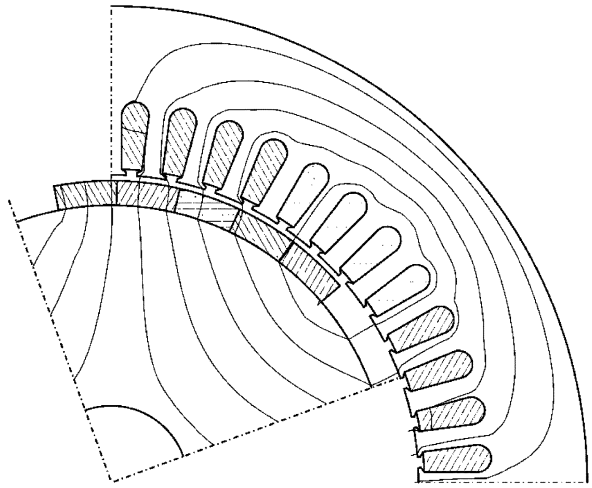

Fig. 9. Motor 1 is a virtual four-pole surface magnet machine. One quarter of the motor was modeled with FEM. There were 1142 elements and 2337 nodes in a second-order finite-element mesh. The main dimensions of the machine are: Stator outer diameter: 310 mm, air-gap diameter: 200 mm, core length: 246 mm.

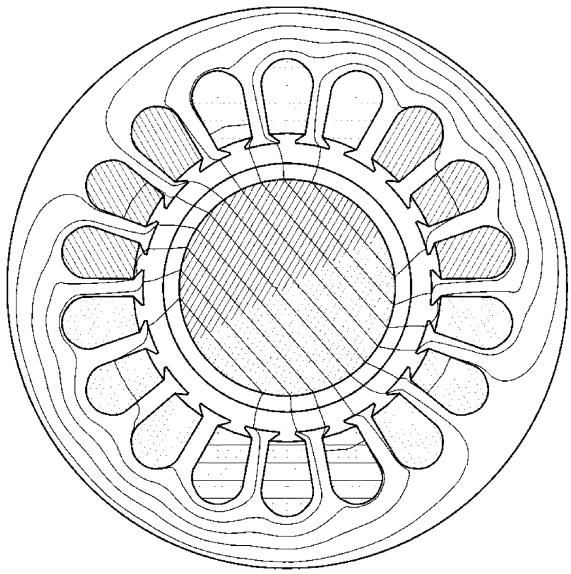

Fig. 10. Motor 2 is a virtual two-pole high-speed machine with a cylindrical magnet covered with stainless steel. A half of the motor was modeled with FEM. There were 1262 elements and 2573 nodes in a second-order finite-element mesh. The main dimensions of the machine are: Stator outer diameter: 70 mm, air-gap diameter: 33.5 mm, core length: 30 mm.

IV. SIMULATION RESULTS

In this section, the difference between the results given by two demagnetization models is demonstrated: one that takes only the antiparallel field into account, and the other one that takes the inclined field into account.

A. Example Machines

Two virtual machines were used in these calculations: A four-pole surface-magnet machine and a two-pole high-speed machine with a stainless steel band over the magnet. The machines are shown in Figs. 9 and 10. The main properties of the machines are given in Table II.

The surface magnet machine is the same machine that was used in paper [2]. One quarter of the machine was modeled using

TABLE III
MODELING CONDITIONS

Situation	Machine 1	Machine 2
Rated torque	255 Nm	1.50 Nm
Overloading torque	525 Nm	1.85 Nm
Rated temperature	100 ºC	100 ºC
Temperature during overloading	150 ºC	170 ºC

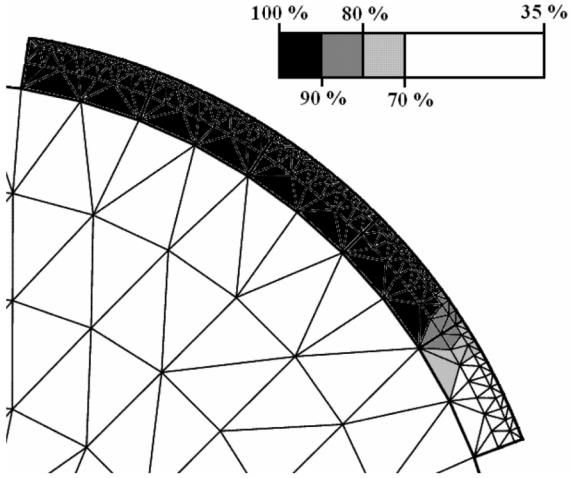

Fig. 11. Relative remaining magnetic polarization inside the magnets of Motor 1 after the heavy loading in an over-temperature. The demagnetization was modeled using the inclined demagnetization model. The direction of the magnetic polarization is radial.

second-order elements for the FEM analysis. The finite-element mesh of the machine contained 1142 elements and 2337 nodes. The magnets were modeled using 245 elements.

A half of the two-pole high-speed machine was modeled using second-order elements. There were 1262 elements and 2573 nodes in the finite-element mesh. The magnet was modeled using 236 elements.

B. Modeling Conditions

The calculations were done assuming that the motors are overheated and heavily loaded. The modeling conditions were selected so that the antiparallel demagnetization model would give a demagnetization between 5% and 10%. The modeling conditions are described in Table III.

First, the no-load voltage was calculated at 100 °C. Then, the machine was run at a constant speed for one period using the exponent function based demagnetization model in overloading condition. After that, the no-load voltage was calculated again at 100 °C. This demagnetization modeling was done both with a model that takes only the antiparallel field into account [2], and a model, which takes an inclined field into account.

C. FEM Calculations

A special program developed in Helsinki University of Technology was used for FEM modeling. The program solves both the field equations and circuit equations simultaneously. The star-connection is taken into account by letting the common point voltage float. Further details of the software can be found in [9].

TABLE IV
COMPUTED RESULTS

Situation	Machine 1 (Surface Magnet Machine) EMF (V) (change)	Machine 2 (High-speed machine) EMF (V) (change)
Healthy machine at 100 ºC	394 V (0 %)	646 V (0 %)
After the overload Anti-parallel demagnetization model [2]	369.7 V (-6.3 %)	615 V (-4.8 %)
After the overload Inclined demagnetization model	369.7 V (-6.3 %)	583 V (-9.7 %)

The demagnetization models were included directly in the program code. The checking for demagnetization is done after each time-step. If there were any demagnetization in any element containing magnetic material, the time-step was recalculated, as described more thoroughly in [2].

D. Results and Discussion

The results of the calculations are presented in Table IV. The results are based on the calculations using second-order elements. The calculations were repeated with third-order elements with the same results. The calculations were also repeated with first-order elements, and in this case there were a bit higher demagnetizations.

It can be seen that the EMF of the surface magnet machine was reduced by 6.3% with both demagnetization models used. The distribution of demagnetization can be seen in Fig. 11. The distribution is the same for both the models used. This is because the demagnetizing field from the stator has a very low inclination when compared to the direction of the magnetic polarization because of the motor geometry.

If it would be necessary to improve the demagnetization resistance of this motor geometry from the modeled kind of demagnetizing situation, it would be possible to use a magnet grade with higher intrinsic coercivity in the trailing edge of the magnet pole, as shown in [10]. This would be very easy from the manufacturing point of view, because the pole is already made using five individual magnet pieces. This kind of design using many magnet grades in one pole is called a “mixed-grade pole.”

The EMF of the two-pole high-speed machine was degreased by some 5% when only the antiparallel demagnetizing field component was considered. When the inclined field was considered in the demagnetization checks, the drop of EMF was some 10%. In both cases, the demagnetization distribution is almost uniform throughout the magnet. There are small areas of higher demagnetization between the poles (Fig. 12).

The significance of the inclined field in demagnetization modeling depends heavily on the machine geometry, as can be understood by comparing the results acquired using the two different machine geometries: With the surface-magnet machine used here, there was practically no difference in the results with different demagnetization models, which means that the demagnetization was completely caused by the antiparallel field. With the two-pole machine studied, the demagnetizing

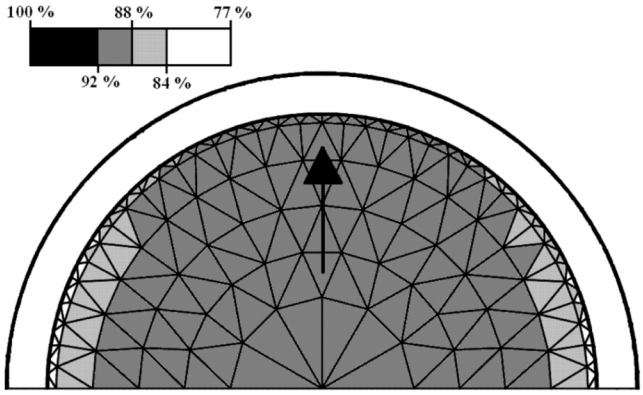

Fig. 12. Relative remaining magnetic polarization inside a magnet of Motor 2 after the heavy loading in an over-temperature. The demagnetization was modeled using the inclined demagnetization model. The arrow shows the direction of magnetic polarization.

field can have a larger angle with the direction of the magnetic polarization, and an inclined field model should be used.

In machine geometries, where the demagnetizing field can have a significant angle with the magnetic polarization vector, the inclined field model should be used. From Fig. 3, it can be seen that even with quite a small field inclination of 20° the inclined field should be taken into account.

V. Conclusion

The behavior of three Nd–Fe–B magnet grades was presented when demagnetizing these samples with an inclined field. It was clearly shown that the inclined field must be taken into account when modeling the demagnetization of axially pressed sintered Nd–Fe–B magnets.

The recoil behavior of sintered Nd–Fe–B magnets was also studied. It can be seen that the recoil curve is not a straight line but curves upwards near the B-axis without forming a minor loop.

Two different PM machines were modeled using an exponential function based demagnetization model considering the inclined field. It was shown that in the demagnetization calculations, where the demagnetizing field can have a large angle between the magnetic polarization vector, it is not enough to consider only the antiparallel demagnetizing field component.

Acknowledgment

This work was supported by Finnish Cultural Foundation, Research Foundation of Helsinki University of Technology, Ulla Tuomisen Säätiö, and High Technology Foundation of Satakunta.

References

[1] K.-C. Kim, S.-B. Lim, D.-H. Koo, and J. Lee, "The shape design of permanent magnet for permanent magnet synchronous motor considering partial demagnetization," *IEEE Trans. Magn.*, vol. 42, no. 10, pp. 3485–3487, Oct. 2006.

[2] S. Ruoho, E. Dlala, and A. Arkkio, "Comparison of demagnetization models for finite-element analysis of permanent-magnet synchronous machines," *IEEE Trans. Magn.*, vol. 43, no. 11, pp. 3964–3968, Nov. 2007.

[3] M. Katter, "Angular dependence of the demagnetization stability of sintered Nd–Fe–B magnets," *IEEE Trans. Magn.*, vol. 41, no. 10, pp. 3853–3855, Oct. 2005.

[4] G. Martinek and M. Kronemüller, "Influence of grain orientation on the coercive field in Fe–Nd–B permanent magnets," *J. Magn. Magn. Mater.*, vol. 86, pp. 177–183, 1991.

[5] W. Fernengel, A. Lehnert, M. Katter, W. Rodewald, and B. Wall, "Examination of the degree of alignment in sintered Nd–Fe–B magnets by measurements of the remanent polarizations," *J. Magn. Magn. Mater.*, vol. 157, pp. 19–20, 1996.

[6] R. Skomski and J. M. D. Coey, *Permanent Magnetism.* College Park, MD: Institute of Physics, 1999, p. 230, ISBN 0-7503-0478-2.

[7] S. Ruoho, "A mathematical method to describe recoil behavior of Nd–Fe–B-material," presented at the Advanced Magnetic Materials and Their Applications 2007, Pori, Finland, 09.10.2007-11.10.2007.

[8] C. L. Harland, L. H. Lewis, Z. Chen, and B.-M. Ma, "Exchange coupling and recoil loop area on $Nd_2Fe_{14}B$ nanocrystalline alloys," *J. Magn. Magn. Mater.*, vol. 271, pp. 53–62, 2004.

[9] A. Arkkio, "Analysis of induction motors based on the numerical solution of the magnetic field and circuit equations," Ph.D. thesis, Univ. Technol., Helsinki, Finland, Sep. 1987.

[10] S. Ruoho and A. Arkkio, "Mixed-grade pole design for permanent magnet synchronous machines," presented at the ACEMP'07 Electromotion'07 Joint Meeting, Bodrum, Turkey, Sep. 10-12, 2007.

Manuscript received November 29, 2007; revised March 25, 2008. Corresponding author: S. Ruoho (e-mail: sami.ruoho@neorem.fi).

Sami Ruoho was born in Pori, Finland, in 1973. He received the M.Sc. degree in applied physics from the University of Turku, Finland, in 1997. He is now pursuing the Ph.D. degree at the Laboratory of Electromechanics, Helsinki University of Technology (TKK). His subject is the modeling of demagnetization of permanent magnets in permanent-magnet machines.

Since 2002, he has been working for Neorem Magnets Oy, a company manufacturing sintered Nd–Fe–B magnets in Finland, as a Research Engineer and as an Application Engineer. During his studies, he still works part time for Neorem Magnets Oy (www.neorem.fi).

Antero Arkkio was born in Vehkalahti, Finland, in 1955. He received the M.Sc. (Tech.) and D.Sc. (Tech.) degrees from Helsinki University of Technology, Finland, in 1980 and 1988, respectively.

He has been a Professor of electrical engineering (Electromechanics) at Helsinki University of Technology (TKK) since 2001. Before his appointment as a Professor, he was a Senior Research Scientist and Laboratory Manager at TKK. He has worked with various research projects dealing with modeling, design, and measurement of electrical machines.